

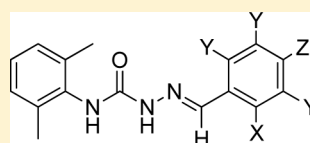
## Structure–Activity Relationship of Semicarbazone EGA Furnishes Photoaffinity Inhibitors of Anthrax Toxin Cellular Entry

Michael E. Jung,<sup>†,‡,\*</sup> Brian T. Chamberlain,<sup>†,‡</sup> Chi-Lee C. Ho,<sup>§</sup> Eugene J. Gillespie,<sup>§</sup> and Kenneth A. Bradley<sup>†,§</sup><sup>†</sup>California NanoSystems Institute, <sup>‡</sup>Department of Chemistry and Biochemistry, <sup>§</sup>Department of Microbiology, Immunology and Molecular Genetics, University of California, Los Angeles, Los Angeles, California 90095, United States

## Supporting Information

**ABSTRACT:** EGA, **1**, prevents the entry of multiple viruses and bacterial toxins into mammalian cells by inhibiting vesicular trafficking. The cellular target of **1** is unknown, and a structure–activity relationship study was conducted in order to develop a strategy for target identification. A compound with midnanomolar potency was identified (**2**), and three photoaffinity labels were synthesized (**3**–**5**). For this series, the expected photochemistry of the phenyl azide moiety is a more important factor than the IC<sub>50</sub> of the photoprobe in obtaining a successful photolabeling event. While **3** was the most effective reversible inhibitor of the series, it provided no protection to cells against anthrax lethal toxin (LT) following UV irradiation. Conversely, **5**, which possessed weak bioactivity in the standard assay, conferred robust irreversible protection vs LT to cells upon UV photolysis.

**KEYWORDS:** Photoaffinity labeling, semicarbazone, aryl azide, anthrax lethal toxin, endosomal trafficking



**1 "EGA":** X, Y = H, Z = Br;  
IC<sub>50</sub> = 1.4 μM  
**2:** X = F, Y = H, Z = Br;  
IC<sub>50</sub> = 0.4 μM

## Photoaffinity probes:

**3:** X = F, Y = H, Z = N<sub>3</sub>; IC<sub>50</sub> = 2.2 μM **NO PHOTOLABELING**  
**4:** X, Y = H, Z = N<sub>3</sub>; IC<sub>50</sub> = 2.8 μM **MODERATE PHOTOLABELING**  
**5:** X, Y = F, Z = N<sub>3</sub>; IC<sub>50</sub> = > 25 μM **BEST PHOTOLABELING**

A common mechanism by which viruses and bacterial toxins enter host cells involves trafficking from an early to a late endosome followed by release into the cytoplasm as triggered by endosomal acidification.<sup>1–3</sup> Inhibition of this process represents a host-targeted strategy for the development of broad-spectrum antiviral and antibacterial drugs. Recently, EGA, *N*<sup>1</sup>-(4-bromobenzylidene)-*N*<sup>4</sup>-(2,6-dimethylphenyl)-semicarbazone, **1**, was identified from a high-throughput phenotypic screen to protect cells from anthrax lethal toxin (LT).<sup>4</sup> Further investigations showed that **1** protected cells from multiple viruses and bacterial toxins that rely on pH-dependent endosomal trafficking to enter cells. Although the details of the biochemical mechanism have been studied, the cellular target(s) remain unknown. We have conducted a structure–activity relationship (SAR) study with the goal of improving the potency of **1** and developing a strategy for photoaffinity labeling and identification of the involved proteins.

A series of derivatives of **1** were synthesized and tested, revealing precise requirements for activity in a tight and relatively flat structure–activity landscape. The 2,6-dimethyl substitution in the *N*<sup>4</sup>-ring as well as an unaltered semicarbazone core were shown to be optimal for activity while certain modifications to the *N*<sup>1</sup>-phenyl ring were tolerated. From the SAR, a compound more potent than the original hit was generated, namely the *N*<sup>1</sup>-2-fluoro-4-bromophenyl analogue (IC<sub>50</sub> = 0.4 μM), **2**. In addition, three photoaffinity probes, **3**–**5**, two of which possess low micromolar activity, were designed and synthesized. Our key finding is that the expected photochemistry of the phenyl azide moiety is a more

important factor than the IC<sub>50</sub> of the photoprobe in achieving successful photolabeling. While **3** was the most potent inhibitor of intoxication by LT in the standard assay, it did not provide protection to the cells upon UV photolysis. Conversely **5**, which possesses two fluorine atoms ortho to the azido function, was a poor inhibitor in the standard assay yet provided cells with the most effective irreversible protection against LT upon UV irradiation. These results represent significant progress toward our goal of identifying the cellular target of this series of compounds and highlight useful considerations for photoaffinity labeling studies in general.

Prior to launching the structure–activity relationship study, we confirmed that the intact semicarbazone structure of **1** was the entity responsible for the inhibition of membrane trafficking. In a previous study, semicarbazones derived from aldehyde-based Cathepsin K inhibitors were shown to have poor C=N bond stability, which, along with other evidence, led researchers to conclude that the semicarbazones were functioning as prodrugs delivering a bioactive aldehyde.<sup>5</sup> On the other hand, structurally distinct peptide-semicarbazones were shown to be stable in acidic media, requiring reflux to induce decomposition.<sup>6</sup> In our case, incubating RAW 264.7 macrophages with the semicarbazone (**6**) and the benzaldehyde component of **1** (both individually and in combination) prior to addition of LT did not prevent toxin-induced cell death,

Received: November 27, 2013

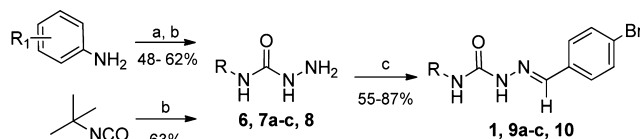
Accepted: December 26, 2013

Published: January 21, 2014

which indicates that the complete semicarbazone structure is required for bioactivity (Supporting Information, Figure 1).

The structure–activity relationship study began by evaluating the importance of the  $N^4$ -2,6-dimethylphenyl moiety for the bioactivity of **1**. Several  $N$ -substituted semicarbazides (**6**, **7a–c**) were synthesized by reaction of hydrazine with an intermediate phenyl carbamate,<sup>7</sup> or *via* direct addition of hydrazine with *tert*-butyl isocyanate (**8**). Condensation of these semicarbazides with 4-bromobenzaldehyde proceeded well in all examples, and the desired products (**1**, **9a–c**, and **10**) were obtained pure by recrystallization (Scheme 1). The stereochemistry of the semicarbazone double bond is assigned as *E* based on analogy with known benzaldehyde semicarbazone structures.<sup>8–12</sup>

### Scheme 1. Synthesis of **1**, **9a–c**, and **10**



Reagents and conditions: (a)  $\text{ClCO}_2\text{Ph}$ ,  $\text{Et}_3\text{N}$ ,  $\text{DCM}$ ,  $\text{rt}$ ; (b)  $\text{NH}_2\text{NH}_2 \cdot \text{H}_2\text{O}$ ,  $\text{DCM}$ ,  $\text{rt}$ ; (c)  $4\text{-BrC}_6\text{H}_4\text{CHO}$ ,  $\text{EtOH}$ ,  $\text{HOAc}$ ,  $\text{reflux}$ . **6** = 2,6-dimethylphenyl semicarbazide, **7a** = 2,4-dimethylphenyl semicarbazide, **7b** = 2,4,6-trimethylphenyl semicarbazide, **7c** = 2,6-diethylphenyl semicarbazide, **8** = *tert*-butyl.

Cell viability data demonstrated the critical importance of the 2,6-dimethylphenyl moiety for the inhibition of membrane trafficking [For the less active analogues, precise  $\text{IC}_{50}$  values were not determined due to poor solubility above  $25 \mu\text{M}$ . These compounds are characterized by an activity limit (i.e.,  $>12.5 \mu\text{M}$ ,  $>25 \mu\text{M}$ ) or as “not protective” if no bioactivity was observed up to  $25 \mu\text{M}$ ] (Table 1). Thus, compounds lacking

**Table 1. Inhibition of LT-Induced Cell Death by **1**, **9a–c**, **10**, and **11****

entry	R	$\text{IC}_{50}$ ( $\mu\text{M}$ )
<b>1</b>	2,6-(Me) <sub>2</sub> C <sub>6</sub> H <sub>3</sub>	$1.4 \pm 0.4$
<b>9a</b>	2,4-(Me) <sub>2</sub> C <sub>6</sub> H <sub>3</sub>	NP
<b>9b</b>	2,4,6-(Me) <sub>3</sub> C <sub>6</sub> H <sub>2</sub>	$12.6 \pm 2.2$
<b>9c</b>	2,6-(Et) <sub>2</sub> C <sub>6</sub> H <sub>3</sub>	$>12.5$
<b>10</b>	<i>t</i> -Bu	NP
<b>11*</b>	Ph	NP

\* $N^1$ -(4-Cl-benzylidene)- $N^4$ -phenylsemicarbazone **11** was obtained commercially and tested previously.<sup>4</sup> Although compound **11** has a 4-Cl substituent rather than a 4-Br one, that difference should not cause a large change in potency (compare activity of **13a** to that of **1**, Table 2). NP = not protective.

this motif (**9a**, **10**, and **11**<sup>4</sup>) were not protective, and a 2,6-diethylphenyl moiety (**9c**) displayed significantly diminished bioactivity ( $\text{IC}_{50} >12.5 \mu\text{M}$ ). Additionally, the  $N^4$ -2,4,6-trimethylphenyl analogue **9b** was approximately 10-fold less active than **1**. Although we did not systematically investigate the activity of analogues with modifications at all the positions of the  $N^4$ -phenyl ring, these results demonstrate the limited potential for modifications in this position of **1**.

Examination of the  $N^1$ -position began with the synthesis and testing of ten compounds prepared from a variety of benzaldehydes (**13a–j**) (Table 2). The bioactivity supported the hypothesis from preliminary SAR work (i.e., **12**)<sup>4</sup> that

**Table 2. Inhibition of LT-Induced Cell Death by **1**, **2**, **12–13ab**, **15**, and **28****

Entry	Structure	$\text{IC}_{50}$ ( $\mu\text{M}$ )
<b>1</b>	Ar = 4-BrC <sub>6</sub> H <sub>4</sub>	$1.4 \pm 0.4$
<b>2</b>	4-Br-2-FC <sub>6</sub> H <sub>3</sub>	$0.4 \pm 0.2$
<b>12*</b>	Ph	NP
<b>13a</b>	4-ClC <sub>6</sub> H <sub>4</sub>	$1.7 \pm 0.2$
<b>13b</b>	(2-Cl-3-CF <sub>3</sub> )C <sub>6</sub> H <sub>3</sub>	NP
<b>13c</b>	2-FC <sub>6</sub> H <sub>4</sub>	$8.2 \pm 1.6$
<b>13d</b>	(3-F-4-Me)C <sub>6</sub> H <sub>3</sub>	$1.8 \pm 0.4$
<b>13e</b>	4-FC <sub>6</sub> H <sub>4</sub>	$7.0 \pm 1.3$
<b>13f</b>	2,4-F <sub>2</sub> C <sub>6</sub> H <sub>3</sub>	$2.1 \pm 0.4$
<b>13g</b>	2,3-(OMe) <sub>2</sub> C <sub>6</sub> H <sub>3</sub>	NP
<b>13h</b>	2,4,6-(OMe) <sub>3</sub> C <sub>6</sub> H <sub>3</sub>	NP
<b>13i</b>	2-MeC <sub>6</sub> H <sub>4</sub>	NP
<b>13j</b>	3-MeC <sub>6</sub> H <sub>4</sub>	$13.4 \pm 1.3$
<b>13k</b>	4-MeC <sub>6</sub> H <sub>4</sub>	$2.9 \pm 0.1$
<b>13l</b>	4-EtC <sub>6</sub> H <sub>4</sub>	$3.0 \pm 0.5$
<b>13m</b>	4- <i>i</i> PrC <sub>6</sub> H <sub>4</sub>	$6.5 \pm 0.6$
<b>13n</b>	4-(OMe)C <sub>6</sub> H <sub>4</sub>	$>12.5$
<b>13o</b>	4-(CCH)C <sub>6</sub> H <sub>4</sub>	$1.7 \pm 0.6$
<b>13p</b>	4-(NHSO <sub>2</sub> Me)C <sub>6</sub> H <sub>4</sub>	NP
<b>13q</b>	4-IC <sub>6</sub> H <sub>4</sub>	$1.8 \pm 0.3$
<b>13r</b>	4-(CF <sub>3</sub> )C <sub>6</sub> H <sub>4</sub>	$2.6 \pm 0.5$
<b>13s</b>	4-CNC <sub>6</sub> H <sub>4</sub>	$2.5 \pm 0.3$
<b>13t</b>	4-Pyridyl	NP
<b>13u</b>	2-Furyl	NP
<b>13v</b>	(5-Br-2-Furyl)	$>25$
<b>13w</b>	2-Thiophenyl	$>25$
<b>13x</b>	(5-Br-2-Thiophenyl)	$1.7 \pm 0.3$
<b>13y</b>	4-Br-2,6-F <sub>2</sub> C <sub>6</sub> H <sub>2</sub>	$4.0 \pm 0.8$
<b>13z</b>	4-Br-2-ClC <sub>6</sub> H <sub>3</sub>	$3.2 \pm 0.1$
<b>13aa</b>	4-Br-3-FC <sub>6</sub> H <sub>3</sub>	$1.5 \pm 0.1$
<b>13ab</b>	4-Br-3-ClC <sub>6</sub> H <sub>3</sub>	$3.4 \pm 0.1$
<b>15</b>		$2.5 \pm 0.6$
<b>28</b>		NP

\*Compound was obtained commercially and tested previously.<sup>4</sup> NP = not protective.

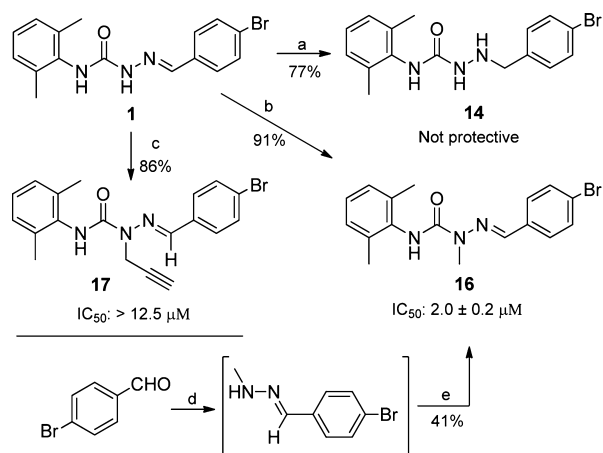
substitution in the 4-position was critical for potency. Next, nine compounds prepared from 4-substituted benzaldehydes were examined in order to give more detailed characterization

of that critical position (13k–s). Although no compound from this set was more potent than 1, substitution in this position was found to be generally well tolerated, with 9 of the 13 compounds featuring a benzylidene motif substituted only in the 4-position registering an  $IC_{50}$  between 1 and 4  $\mu M$ . Five analogues consisting of heterocyclic rings were also synthesized. While 13t–13w did not offer protection to cells challenged with LT, the 5-bromothiophen-2-ylmethylene example (13x) possessed bioactivity similar to that of 1 ( $IC_{50}$  1.7  $\mu M$  and 1.4  $\mu M$ , respectively).

The fact that the  $N^1$ -2,4-difluoro analogue (13f) was notably more potent than the analogue from 4-fluorobenzaldehyde (13e) ( $IC_{50}$  = 2.1  $\mu M$  vs  $IC_{50}$  = 7.0  $\mu M$ ) led us to examine whether including a fluorine in the 2-position of the  $N^1$ -ring would similarly augment the potency of 1. Indeed, compound 2 displayed a significant increase in activity ( $IC_{50}$  = 0.4  $\mu M$ ). Encouraged by this result, we synthesized and tested compounds 13y–13ab, which gave  $IC_{50}$  values that were all larger than the original lead compound 1.

The effects of modifications made to the semicarbazone core are compiled in Scheme 2. The imine bond of 1 could be

### Scheme 2. Synthesis and Bioactivity of 14, 16, and 17

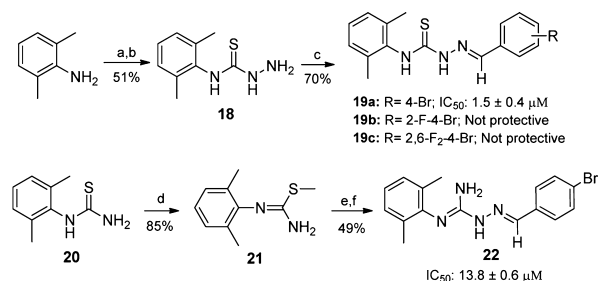


Reagents and conditions: (a)  $BH_3$ , THF, 50  $^{\circ}C$ ; (b) MeI,  $K_2CO_3$ , DMF, rt; (c)  $BrCH_2CCH$ ,  $K_2CO_3$ , DMF, rt; (d) MeNHNH $_2$ ·H $_2$ O, EtOH, reflux; (e) Ph 2,6-Me $_2$ phenyl carbamate, Et $_3$ N, DCM, rt.

effectively reduced to the disubstituted hydrazine derivative (14) using an excess of borane in THF with heating. The compound was not protective at the concentrations tested. The 1-(4-bromophenyl)ethylidene analogue (15) was synthesized by the condensation of the semicarbazide 6 with 4'-bromoacetophenone. This change caused a minor reduction in potency, with 15 showing an  $IC_{50}$  of 2.5  $\mu M$  (Table 2). The semicarbazone core of 1 could be methylated with high regioselectivity by treatment with iodomethane and  $K_2CO_3$  in DMF to give 16. Synthesis of 16 via addition of methyl hydrazine to 4-bromobenzaldehyde followed by reaction with phenyl (2,6-dimethylphenyl)carbamate gave a product with identical  $^1H$  NMR and  $^{13}C$  NMR spectra and thus confirmed the regiochemistry of methylation at the  $N^2$ -position. The bioactivity of 16 was not significantly affected compared to that of 1 ( $IC_{50}$  = 2.0  $\mu M$  and 1.4  $\mu M$ , respectively). Incorporating a propargyl group into this position by alkylation with propargyl bromide generated 17, which had somewhat impaired bioactivity ( $IC_{50}$  > 12.5  $\mu M$ ).

The thiosemicarbazones (19a–c) were synthesized from  $N$ -2,6-dimethylphenyl thiosemicarbazide, 18, and the corresponding benzaldehyde in refluxing ethanol and acetic acid<sup>13</sup> (Scheme 3). Substituting the carbonyl of 1 with a thiocarbonyl,

### Scheme 3. Synthesis and Bioactivity of 19a–c and 22



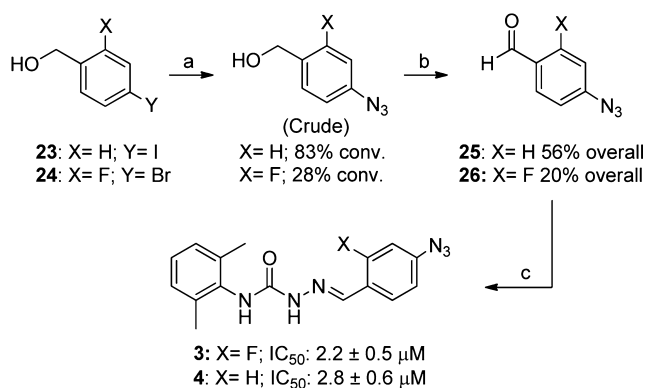
Reagents and conditions: (a)  $CS_2$ , NaOH, DMF; (b)  $NH_2NH_2$ ·H $_2$ O, DMF, 60  $^{\circ}C$ ; (c) 4- $BrC_6H_4CHO$ , EtOH, HOAc, reflux; (d) MeI, EtOH, reflux,  $Na_2CO_3$ ; (e)  $NH_2NH_2$ ·H $_2$ O, EtOH, HOAc, reflux; (f) 4- $BrC_6H_4CHO$ , EtOH, HOAc, reflux.

19a, had little effect on the potency of the compound ( $IC_{50}$  = 1.5  $\mu M$ ) while exacerbating an already problematic solubility profile. For example, compounds 19b and 19c were poorly soluble at assay concentrations (cLogP: 19a, 5.8; 19b, 6.0; 19c, 6.1; 1, 5.2) and did not return meaningful dose–response curves. A significantly more soluble  $C=NH$  compound (22) (cLogP: 3.9–4.0) was elaborated from the  $S$ -methylation of (2,6-dimethylphenyl)thiourea,<sup>14</sup> 20, to give 21, followed by displacement with hydrazine and condensation with 4-bromobenzaldehyde to give the hydrazinecarboximidamide, 22. Unfortunately, the bioactivity of this compound was diminished ( $IC_{50}$  = 13.8  $\mu M$ ).

From the structure–activity relationship data, it was evident that the most effective photoaffinity probe would contain an  $N^4$ -2,6-dimethylphenyl unit, an unmodified semicarbazone core, and a 4-substituted benzylidene motif at the  $N^1$ -position. As the course of phenyl azide photolysis is known to be sensitive to the substituents of the phenyl azide,<sup>15,16</sup> three photoaffinity labels were designed. The first, 3, would be predicted by the SAR to provide the highest potency in the *in vitro* assay. The second, 4, would consist of a simple phenyl azide commonly employed in the biochemical literature.<sup>17</sup> The third molecule, 5, would flank the azido group with fluorines, a modification known to give a longer-lived singlet nitrene that can more effectively yield genuine insertion products upon photolysis.<sup>18,19</sup>

Compounds 3, 4, and 5 were synthesized from 6 and the desired azido-containing benzaldehyde (4-azidobenzaldehyde (25), 4-azido-2-fluorobenzaldehyde (26), and 4-azido-2,3,5,6-tetrafluorobenzaldehyde (27)), in the usual manner. Compound 25 could be obtained from the ethylene acetal of 4-nitrobenzaldehyde via catalytic hydrogenation and diazotization followed by reaction with sodium azide.<sup>20</sup> In this study we chose to perform an Ullmann-type coupling with 4-iodobenzyl alcohol (23) and sodium azide<sup>21</sup> followed by oxidation to the aldehyde (Scheme 4). This protocol was convenient on the milligram scale and provided access to the previously undescribed 26 from 4-bromo-2-fluorobenzyl alcohol, 24. Compound 27 was synthesized according to a known procedure via an  $SNAr$  reaction of sodium azide with pentafluorobenzaldehyde.<sup>18</sup>

## Scheme 4. Synthesis and Bioactivity of Photoaffinity Probes 3 and 4



Reagents and conditions: (a) NaN<sub>3</sub>, CuI, MeHNCH<sub>2</sub>CH<sub>2</sub>NHMe, Na ascorbate, DMSO/H<sub>2</sub>O; (b) PCC, DCM, rt; (c) **6**, EtOH, HOAc, reflux.

As predicted, **3** and **4** were inhibitors of LT membrane trafficking, with **4** having an IC<sub>50</sub> of 2.8 μM and **3** giving an IC<sub>50</sub> of 2.2 μM, while **5** was only weakly protective against LT, beginning to show a biological effect at 25 μM. The reversibility of inhibition by **3–5** was confirmed by incubating cells with inhibitor-containing media and then exchanging it for fresh media prior to intoxication with LT. As expected, the arylsemicarbazones could be “washed-out” and there was no cell viability in these experiments upon exposure to LT (Figure 1). Irradiating the cell cultures incubated with **4** and **5** with 5

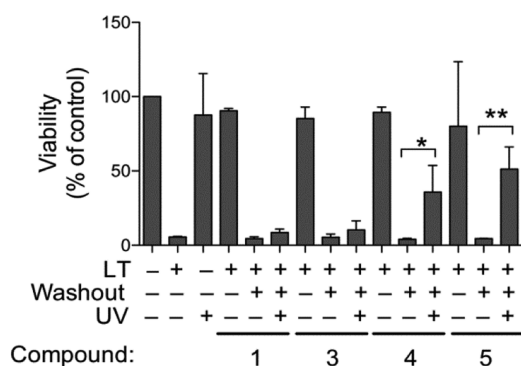


**Figure 1.** Photoaffinity labeling of RAW264.7 cells with aryl azide photoprobes. LT = Anthrax lethal toxin, UV = 5 min ultraviolet (UVB) irradiation, “washout” indicates replacing cell media with fresh media lacking **1**, **3**, **4**, or **5** prior to intoxication with LT. Compounds **4** and **5** provided statistically significant protection (\* =  $p < 0.05$ , \*\* =  $p < 0.01$ ) following photoirradiation vs washout.

min of ultraviolet (UVB) light prior to media exchange conferred significant protection on cells against LT. Compound **3** did not offer statistically significant protection after UVB photolysis and media exchange. The irreversible protection provided to cells upon the irradiation of **4** and **5** implies that these compounds form covalent linkages with the target protein upon exposure to UVB light.

A common strategy for identifying proteins bound by photoaffinity probes is to incorporate an alkynyl moiety into the photoaffinity probe that can be conjugated with an azido-containing fluorescent dye following cell lysis.<sup>22</sup> Given the low activity of **17** and the limited potential for making modifications

in the *N*<sup>4</sup>-phenyl ring, it is not apparent how such a “clickable” linker could be included into a bioactive photoaffinity version of **1**. Nevertheless, the convenience of this approach led us to synthesize compound **28**, an *N*<sup>2</sup>-propargyl analogue of **4** (Table 2). This compound did not offer any protection to cells at any concentration tested. Accordingly, radiolabeled versions of **5** are being considered as a means of identifying the bound proteins.

In conclusion, we have conducted a structure–activity relationship study that has examined how modifications in the structure of **1** affect the cellular entry of LT. The data indicate a tight and relatively flat SAR, with many of the original structural features of **1** being preferred for bioactivity. Inclusion of a fluorine in the 2-position of the *N*<sup>1</sup>-benzylidene portion appears to be a general strategy for increasing the potency of these arylsemicarbazones and, in the case of **2**, improved potency to midnanomolar levels. The photoaffinity probes **3**, **4**, and **5** were synthesized from azido-containing benzaldehydes. Photolysis of **4** and **5** in the presence of RAW 264.7 cells conferred irreversible resistance to LT and implies that covalent bonds with the cellular target were generated. We are in the process of designing and preparing radiolabeled versions of these compounds to facilitate target identification.

## ■ ASSOCIATED CONTENT

## S Supporting Information

Synthetic procedures and <sup>1</sup>H NMR, <sup>19</sup>F NMR (when applicable), and HRMS characterization data for all compounds tested in bioassay. For select compounds, additional characterization includes <sup>13</sup>C NMR (**2**, **3**, **4**, **13x**, **14**, **15**, **16**, **17**, **19a**, **28**), FTIR (**2–5**, **13x**, **28**), and melting point (**2**, **13x**). NMR spectra are provided for select compounds. Materials and methods for cellular intoxication assays and photolabeling experiments are included. This material is available free of charge via the Internet at <http://pubs.acs.org>.

## ■ AUTHOR INFORMATION

## Corresponding Author

\*E-mail: [jung@chem.ucla.edu](mailto:jung@chem.ucla.edu).

## Notes

The authors declare no competing financial interest.

## ■ REFERENCES

- (1) Di Simone, C.; Zandonatti, M. A.; Buchmeier, M. J. Acidic pH Triggers LCMV Membrane Fusion Activity and Conformational Change in the Glycoprotein Spike. *Virology* **1994**, *198*, 455–465.
- (2) Knodler, L. A.; Celli, J.; Finlay, B. B. Pathogenic trickery: deception of host cell processes. *Nat. Rev. Mol. Cell Biol.* **2001**, *2*, 578–588.
- (3) White, J.; Matlin, K.; Helenius, A. Cell fusion by Semliki Forest, influenza, and vesicular stomatitis viruses. *J. Cell Biol.* **1981**, *89*, 674–679.
- (4) Gillespie, E. J.; Ho, C.-L.; Balaji, K.; Li, Z.; Thomas, D.; Clemens, D. L.; Deng, G.; Wang, Y.; Elsaesser, H.; Tamilselvam, B.; France, B.; Chamberlain, B. T.; Blanke, S. R.; Cheng, G.; Brooks, D.; Jung, M. E.; Manchester, M.; Zink, J.; Colicelli, J.; Damoiseaux, R.; Bradley, K. A. Selective Inhibitor of Endosomal Trafficking Pathways Exploited by Multiple Toxins and Viruses. *Proc. Natl. Acad. Sci. U.S.A.*, early ed.; **2013** (Nov 4 2013); pp 1–9.
- (5) Adkison, K. K.; Barrett, D. G.; Deaton, D. N.; Gampe, R. T.; Hassell, A. M.; Long, S. T.; McFadyen, R. B.; Miller, A. B.; Miller, L. R.; Payne, J. A.; Shewchuk, L. M.; Wells-Knecht, K. J.; Willard, D. H.; Wright, L. L. Semicarbazone-based inhibitors of cathepsin K, are they



prodrugs for aldehyde inhibitors? *Bioorg. Med. Chem. Lett.* **2006**, *16*, 978–983.

(6) Leban, J.; Blisse, M.; Krauss, B.; Rath, S.; Baumgartner, R.; Seifert, M. H. J. Proteasome inhibition by peptide-seimcarbazonen. *Bioorg. Med. Chem.* **2008**, *16*, 4579–4588.

(7) Yogeeswari, P.; Sriram, D.; Thirumurugan, R.; Raghavendran, J. V.; Sudhan, K.; Pavana, R. K.; Stables, J. Discovery of *N*-(2,6-Dimethylphenyl)-Substituted Semicarbazones as Anticonvulsants: Hybrid Pharmacophore-Based Design. *J. Med. Chem.* **2005**, *48*, 6202–6211.

(8) Sarojini, B. K.; Narayana, B.; Bindya, S.; Yathirajan, H. S.; Bolte, M. 4-(Methylthio)benzaldehyde semicarbazone. *Acta Crystallogr., Sect. E: Struct. Rep. Online* **2007**, *E63*, o2946.

(9) Naik, D. V.; Palenik, G. J. The crystal and molecular structures of acetone semicarbazone and benzaldehyde semicarbazone. *Acta Crystallogr., Sect. B* **1974**, *30B*, 2396–2401.

(10) Basuli, F.; Peng, S.-M.; Bhattacharya, S. Chemical Control on the Coordination Mode of Benzaldehyde Semicarbazone Ligands. Synthesis, Structure, and Redox Properties of Ruthenium Complexes. *Inorg. Chem.* **2001**, *40*, 1126–1133.

(11) Casas, J. S.; Garcia-Tasende, M. S.; Sordo, J. Main group metal complexes of semicarbazones and thiosemicarbazones. A structural review. *Coord. Chem. Rev.* **2000**, *209*, 197–261.

(12) Lin, L.; Fan, W.; Chen, S.; Ma, J.; Hu, W.; Lin, Y.; Zhang, H.; Huang, R. Photochromism of (E)-4-phenyl-1-(pyridine-2-ylmethylene)semicarbazide. *New J. Chem.* **2012**, *36*, 2562–2567.

(13) Tripathi, L.; Kumar, P.; Singh, R.; Stables, J. P. Design, synthesis and anticonvulsant evaluation of novel *N*-(4-substituted phenyl)-2-[4-(substituted) benzylidene]hydrazinecarbothio amides. *Eur. J. Med. Chem.* **2012**, *47*, 153–166.

(14) Rasmussen, C. R.; Villani, F. J., Jr.; Weaner, L. E.; Reynolds, B. E.; Hood, A. R.; Hecker, L. R.; Nortey, S. O.; Hanslin, A.; Costanzo, M. J.; Powell, E. T.; Molinari, A. J. Improved Procedures for the Preparation of Cycloalkyl-, Arylalkyl-, and Arylthioureas. *Synthesis* **1988**, 456–459.

(15) Gritsan, N. P.; Platz, M. S. Kinetics, Spectroscopy, and Computational Chemistry of Arylnitrenes. *Chem. Rev.* **2006**, *106*, 3844–3867.

(16) Li, Y. Z.; Kirby, J. P.; George, M. W.; Poliakoff, M.; Schuster, G. B. 1,2-Didehydroazepines from the Photolysis of Substituted Aryl Azides: Analysis of Their Chemical and Physical Properties by Time-Resolved Spectroscopic Methods. *J. Am. Chem. Soc.* **1988**, *110*, 8092–8098.

(17) Kotzyba-Hibert, F.; Kapfer, I.; Goeldner, M. Recent Trends in Photoaffinity Labeling. *Angew. Chem., Int. Ed. Engl.* **1995**, *34*, 1296–1312.

(18) Keana, J. F. W.; Cai, S. X. New Reagents for Photoaffinity Labeling: Synthesis and Photolysis of Functionalized Perfluorophenyl Azides. *J. Org. Chem.* **1990**, *55*, 3640–3647.

(19) Schnapp, K. A.; Poe, R.; Leyva, E.; Soundararajan, N.; Platz, M. S. Exploratory Photochemistry of Fluorinated Aryl Azides. Implications for the Design of Photoaffinity Labeling Reagents. *Bioconjugate Chem.* **1993**, *4*, 172–177.

(20) Walton, R.; Lahti, P. M. An Efficient Simple Synthesis of 4-Azidobenzaldehyde. *Synth. Commun.* **1998**, *28*, 1087–1092.

(21) Andersen, J.; Madsen, U.; Bjorkling, F.; Liang, X. Rapid Synthesis of Aryl Azides from Aryl Halides under Mild Conditions. *Synlett* **2005**, 2209–2213.

(22) Lapinsky, D. J. Tandem photoaffinity labeling–bioorthogonal conjugation in medicinal chemistry. *Bioorg. Med. Chem.* **2012**, *20*, 6237–6247.